

Regional patterns and asynchronous onset of recent ice-wedge degradation in arctic Alaska

Gerald V. Frost^{1*}, Tracy Christopherson², Anna Liljedahl³, Matthew J. Macander¹, Donald A. Walker⁴ and Aaron F. Wells²

¹ABR, Inc. – Environmental Research and Services, Inc., Fairbanks, AK
²ABR, Inc. – Environmental Research and Services, Inc., Anchorage, AK
³Water and Environmental Research Center, University of Alaska Fairbanks
⁴Alaska Geobotany Center, University of Alaska Fairbanks
 *corresponding author <jfrost@abrinc.com>



Poster ID C21C-750

Abstract

Ice-wedge polygons are conspicuous and widespread in arctic landscapes, creating complex microtopography and strong, meter-scale contrasts in hydrology, soil, vegetation, and ground ice conditions. Thaw of the upper portion of ice-wedges results in ground subsidence (thermokarst), plant mortality and the formation of small, flooded pits along the polygon margins. Secondary impacts, such as changes in flowpaths, spatially-variable flooding and drainage of polygon centers, and thermal erosion of permafrost, extend well beyond the thermokarst pits themselves. We delineated small waterbodies in historical airphotos and modern high-resolution satellite imagery and made ground observations across a network of 45 km² study areas spanning the western and central regions of Alaska's North Slope. The imagery archive covers three epochs: 1948–1955, 1979–1985, and 2009–2012. Our analysis focused on residual upland surfaces dominated by Holocene-aged ice wedges, where surface water is mainly restricted to degraded ice-wedges. Total extent of flooded pits increased at most landscapes since circa 1980 (range -27 – +135%; median +10.6%). An intriguing regional pattern was evident: degradation of Holocene ice-wedges was already well underway by 1950 across much of the western North Slope, but degradation initiated much more recently on eolian sand and silt (yedoma) deposits prevalent to the east. Our results indicate that recent degradation of Holocene ice wedges across northern Alaska cannot be explained by late-20th century warmth alone. Possible mechanisms for earlier onset of degradation on the western North Slope include differences in recent climate history, snow regime, and thermal and physical properties of surficial materials. These findings provide context for interpreting and predicting ice-wedge thermokarst processes, thresholds, and impacts in Alaska and elsewhere in the circumpolar arctic.

Introduction & Methods

Numerous reports of ice-wedge thermokarst have emerged over the last decade from across the Pan-Arctic, including the Alaska North Slope (Jorgenson et al. 2006), as well as northern Canada and Siberia (Liljedahl et al., in revision). Here we evaluate regional patterns of ice-wedge degradation across the Alaska North Slope, where ice-wedge polygons are widespread and conspicuous, and for which extensive archives of historical high-resolution photography exist to identify spatio-temporal dynamics in polygonal landscapes for three epochs: circa 1950, 1982, and 2010. The study areas include three geomorphic environments with differing substrates, landscape histories, and ground ice conditions: (1) alluvio-marine deposits along the Chukchi Sea coast; (2) the eolian sand sheet in the central coastal plain; and (3) yedoma uplands (ice-rich eolian silt) of the northern foothills (Fig. 1).

We quantified the extent of thaw pits in polygonal terrain (Figs. 2–3) in high-resolution imagery for each epoch across a network of eleven 15 km² study areas spanning the National Petroleum Reserve–Alaska. We focused on residual upland surfaces, where ice wedges have developed over long periods of time and where small waterbodies are generally restricted to thermokarst pits. We used an extensive ground data set to partition upland landscapes by geomorphic unit (alluvio-marine deposits, eolian sand sheet, and yedoma) and by polygon type (high-center, low-center, mixed high- and low-center, and mixed pit and polygon complex). To distinguish thermokarst pits, we first extracted dark reflectance values in panchromatic (circa 1950) imagery and color-infrared (circa 1982 and 2010) imagery using a spectral thresholding approach. Dark reflectance pixels were then converted to shapes in GIS. For areas with flooded low-center polygons, we distinguished thaw pits from flooded polygon centers based on the ratio of shape length to shape area; this ratio is typically much higher for thaw pits, which have convoluted outlines but small total area.

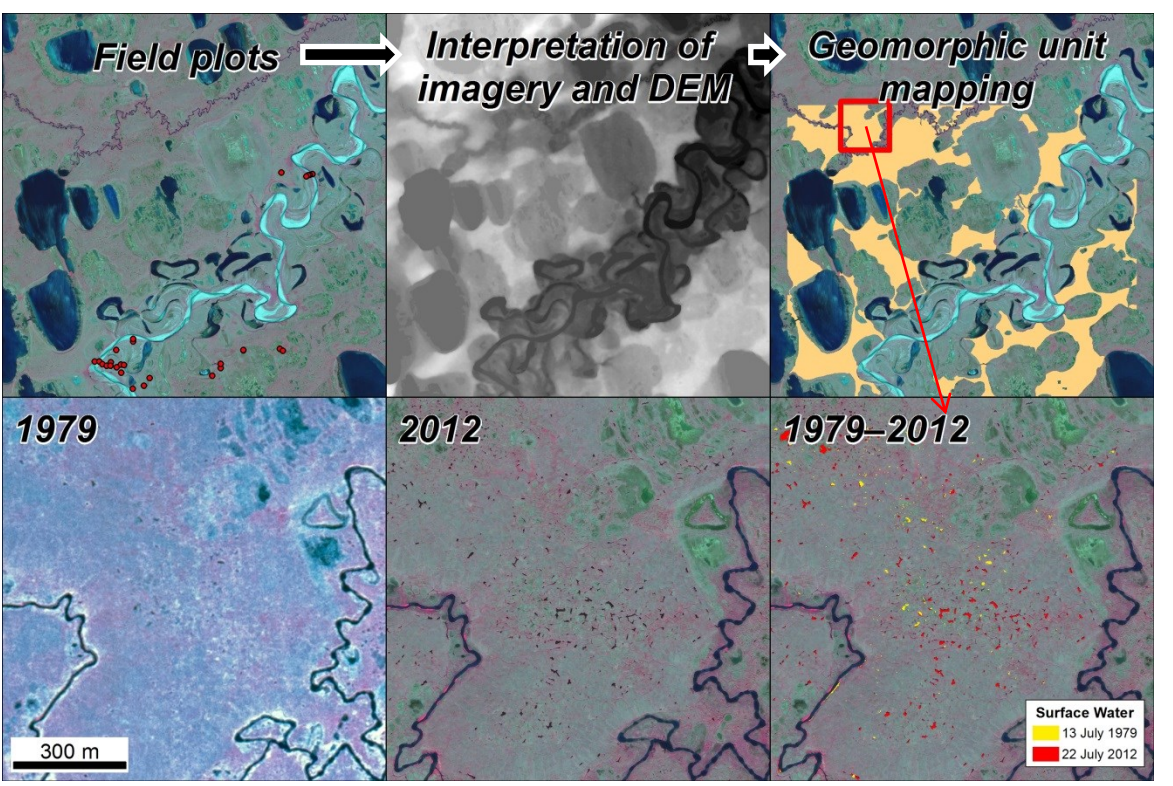


Fig. 2. Example of processing steps for identification of thaw pits on eolian sand sheet uplands at the Judy Creek site. Field observations of vegetation, landforms, and soils informed the mapping of residual upland surfaces. Surface water was then delineated for each epoch within areas mapped as residual upland.

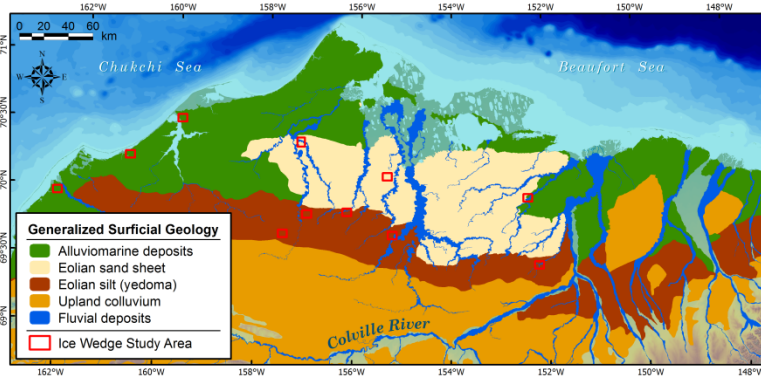


Fig. 1. Study sites (red boxes) encompass residual uplands corresponding to three geomorphic environments: alluvio-marine deposits, eolian sand sheet, and yedoma. Mapping after Jorgenson and Grunblatt (2013).

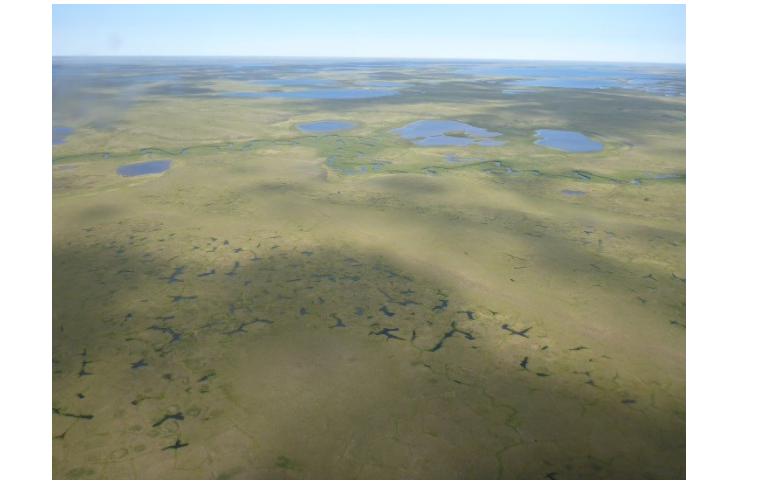


Figure 3. Aerial (above) and ground (below) views of degraded ice-wedge terrain at Oumalik River site. Degradation triggers ground subsidence, vegetation mortality, ponding, and the alteration of hydrologic flowpaths.



Results

Spatio-temporal analysis revealed increases in the total area of flooded thaw pits at 7 of 11 study landscapes since circa 1950 (Table 1, Fig. 4). However, pit extent decreased at the three westernmost sites dominated by alluvio-marine deposits, where thaw pits were already abundant by 1949; changes since then primarily reflect pit stabilization and the development of wetland vegetation in the thaw pits (see Fig. 9 at right).

Pit extent increased since circa 1950 at all five yedoma sites. However, the extent of thaw pits in yedoma is low at most sites relative to the alluvio-marine sites. There is also some evidence of a west-to-east gradient in the timing of degradation in yedoma and sand sheet soils, with more recent onset evident at eastern sites.

Table 1. Summary of study area and imagery attributes.

Study area	Geomorphic unit(s)	Lat (°N)	Long (°W)	Imagery date by epoch		
				1950	1982	2010
Kugachiak	Alluvio-marine + yedoma	70.0	162.3	26 Jun 1955	16 Jul 1982	8 Aug 2010 (GE1)
Ongorakvik	Alluvio-marine	70.3	160.9	26 Jun 1955	2 Aug 1985	5 Jul 2012 (WV2)
Wainwright	Alluvio-marine	70.6	159.8	1 July 1949	18 Jul 1982	8 Jul 2012 (WV2)
U. Meade	Yedoma	69.8	157.5	12 July 1949	16 Jul 1982	19 Jul 2009 (GE1)
Atkasuk	Sand sheet	70.5	157.2	26 Jun 1955	2 Aug 1985	22 Jul 2012 (GE1)
Piksiksak	Yedoma	70.0	157.0	23 Jul 1955	16 Jul 1982	22 Jul 2012 (GE1)
Topagoruk	Yedoma	70.0	156.2	23 Jul 1955	16 Jul 1982	9 Jul 2010 (GE1)
Oumalik R.	Sand sheet	70.3	155.4	25 Jul 1955	16 Jul 1982	15 Jul 2009 (GE1)
Titiluk	Yedoma	69.8	155.2	1 Aug 1948	16 Jul 1982	25 Jun 2010 (WV2)
Judy Creek	Sand sheet	70.1	152.4	24 Jul 1955	13 Jul 1979	22 Jul 2012 (GE1)
Kogosukruk	Sand sheet + yedoma	69.6	152.2	23 Jul 1955	1 Aug 1977	22 Aug 2011 (WV2)

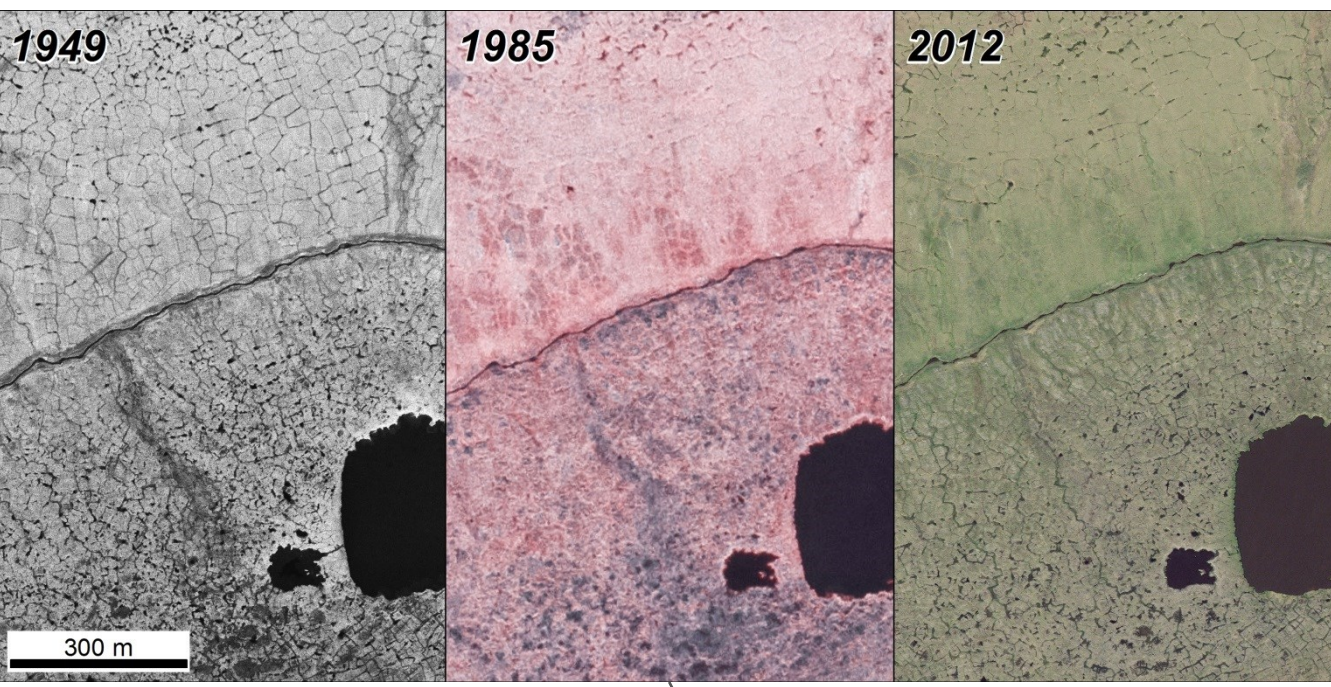


Figure 5. Thaw pit evolution at Ongorakvik study area, 1949–2012. Ice-wedge degradation was already widespread at all 3 Chukchi coastal sites by circa 1950 and changes since then primarily reflect pit stabilization.

Figure 6. Thaw pit development at Kugachiak site on remnant yedoma uplands (top half of images) and on alluvio-marine deposits (bottom). In 1955, few thaw pits were evident on yedoma but pits were numerous in alluvio-marine deposits. Pit extent peaked around 1980. Subsequent changes primarily reflect vegetation recovery and pit stabilization; note revegetation of many pits in yedoma in the 2010 CIR image. However, large deep pits can be persistent (yellow arrows), likely due to lack of vegetation recovery in deep pits.

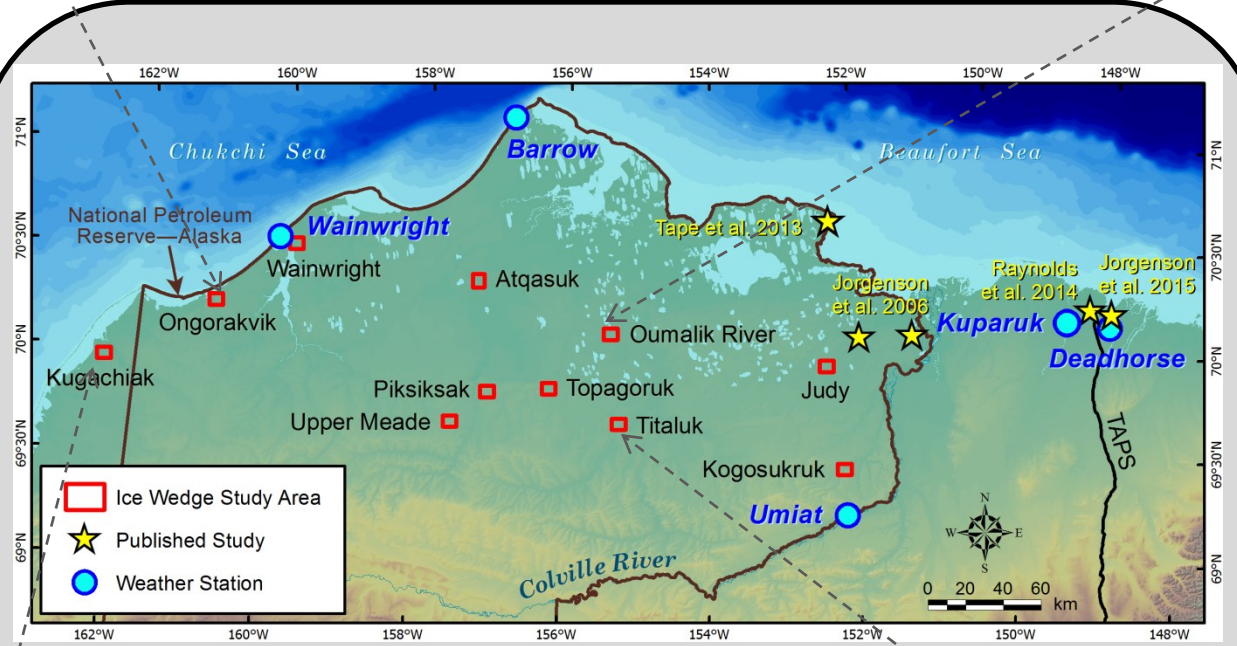
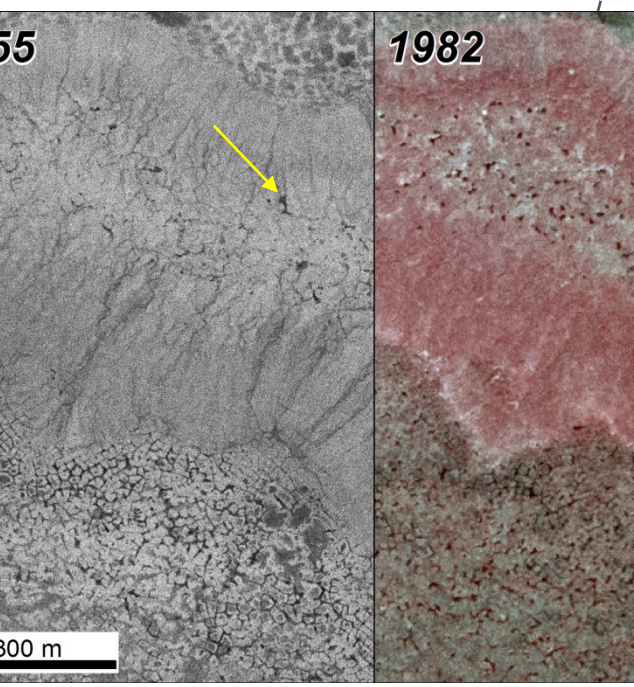


Figure 7. Thermokarst pit development on eolian sand sheet at Oumalik River study area, 1948–2009. Scattered pits are evident in the 1948 and 1982 imagery, but most surface water is associated with the centers of low-centered polygons. Many large pits had developed by 2009. The overall extent of thaw pits is generally lowest on eolian sand deposits, which accumulate ground-ice at relatively low rates.

Figure 8. Recent onset of ice-wedge degradation in yedoma uplands of Titiluk site. Virtually no pits are evident in the 1948 photo. Initiation and growth of thermokarst pits accelerated dramatically after 1982.

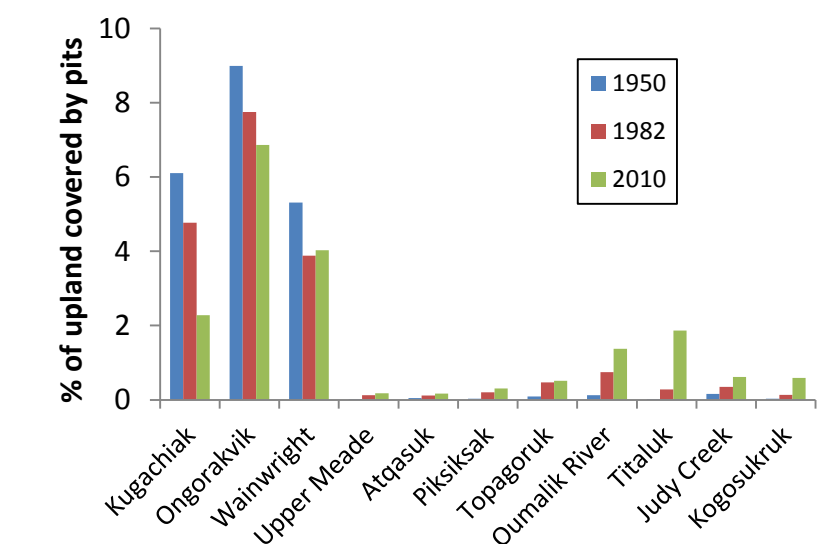


Figure 4. (above) Percent of residual upland area covered by flooded thaw pits for the three epochs. Sites are ordered from west to east. (below) Rate of change in pit extent at yedoma sites across each epoch.

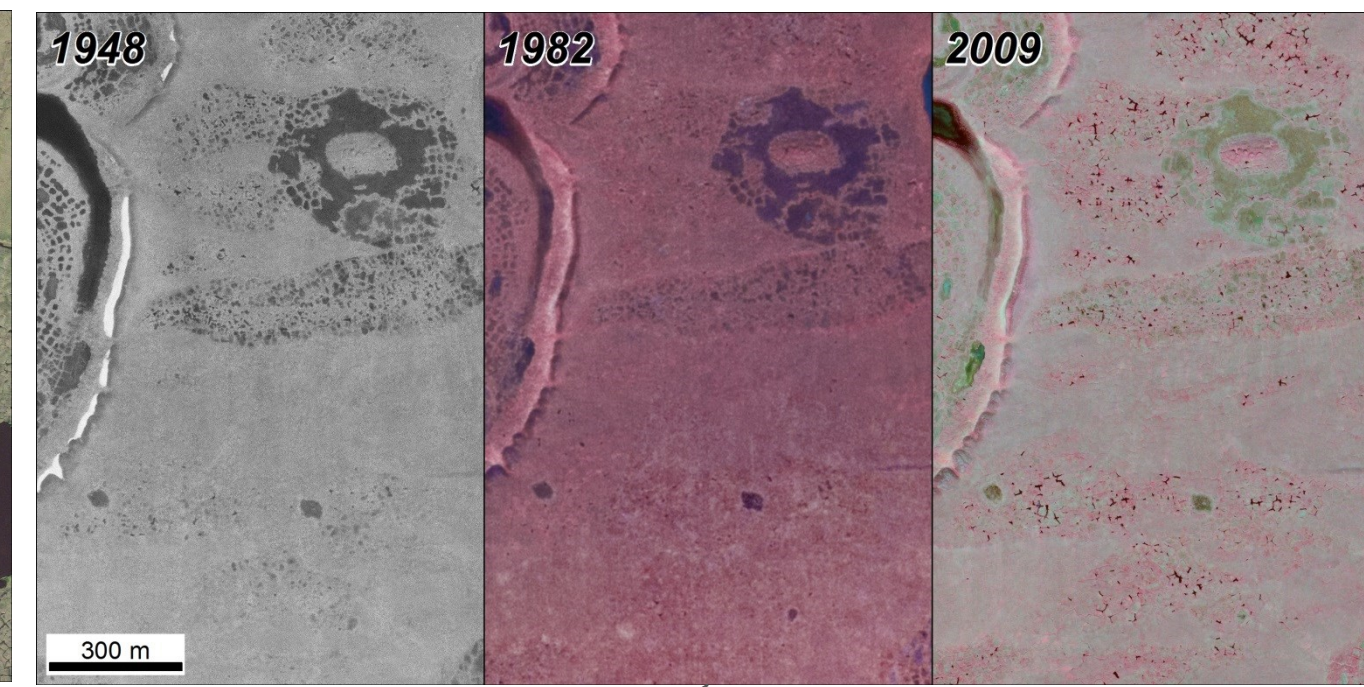
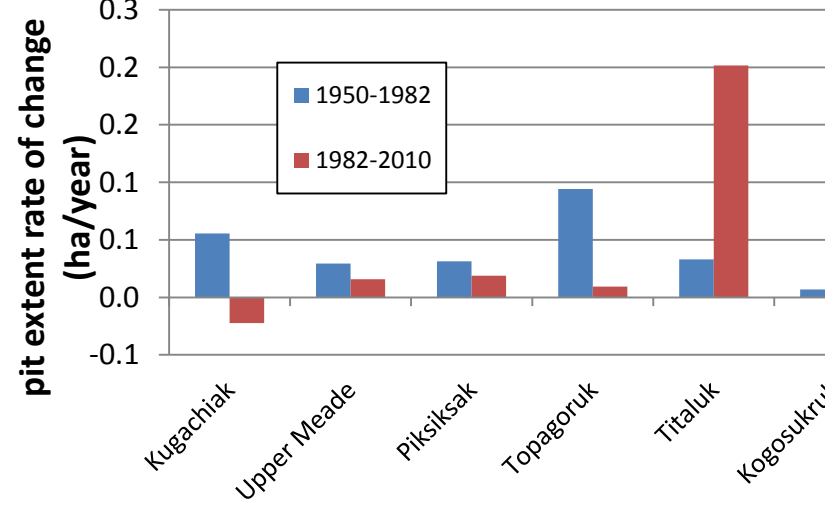


Figure 7. Thermokarst pit development on eolian sand sheet at Oumalik River study area, 1948–2009. Scattered pits are evident in the 1948 and 1982 imagery, but most surface water is associated with the centers of low-centered polygons. Many large pits had developed by 2009. The overall extent of thaw pits is generally lowest on eolian sand deposits, which accumulate ground-ice at relatively low rates.

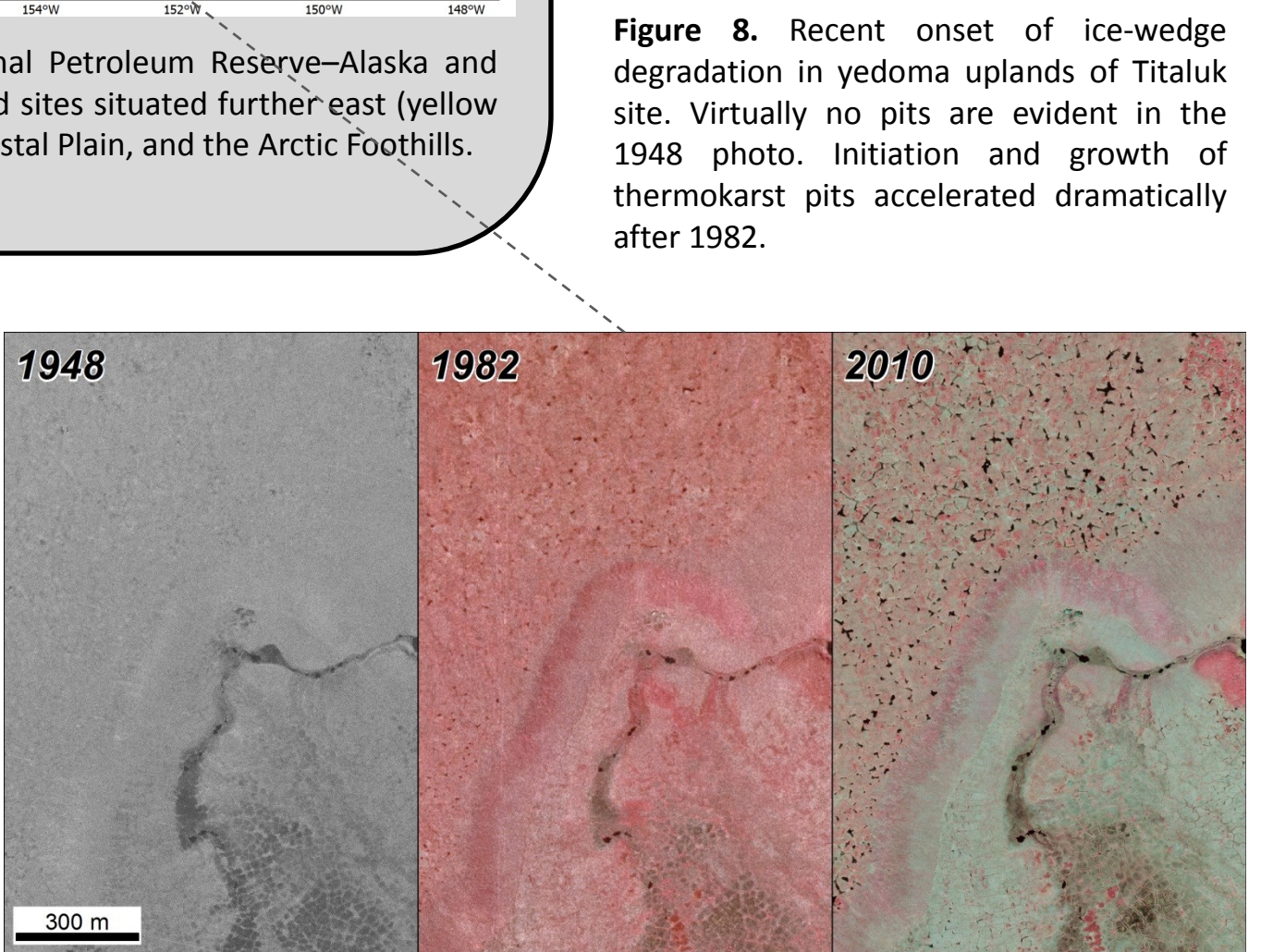


Figure 8. Recent onset of ice-wedge degradation in yedoma uplands of Titiluk site. Virtually no pits are evident in the 1948 photo. Initiation and growth of thermokarst pits accelerated dramatically after 1982.

Discussion

Degradation of western alluvio-marine deposits occurred earliest. These deposits are older than Pleistocene-aged sand sheet and yedoma soils, and may have undergone earlier cycles of degradation, stabilization, and growth of secondary ice-wedge growth. Warming since the Little Ice Age may explain the abundance of thaw pits by 1949. Degradation in yedoma soils is comparatively recent. Silty soils favor accumulation of segregated ice at the base of the active-layer ("intermediate layer" of Shur et al. 2005) which helps to protect underlying ice wedges. High biomass plant communities on yedoma soils (e.g., shrub-tussock tundra) also protect permafrost from thawing. Degradation in sand sheet soils is rather variable; ground-ice accumulation is slowest in sandy soils. However, ice-poor intermediate layers provide little protection. Although we only quantified changes in surface water extent, the secondary impacts of ice-wedge degradation extend well beyond the footprints of thermokarst pits themselves. Changes in the relative elevation of polygon troughs usually results in complex patterns of drying in some areas (e.g., greater connectivity of polygon troughs) and wetting in others (redirection of flow paths) (Fig. 9).



Figure 9. Aerial view of pock-marked thermokarst pit complex at Wainwright. Dense high-centered polygons are separated by deep troughs, many of which now support dense hydrophytic vegetation.

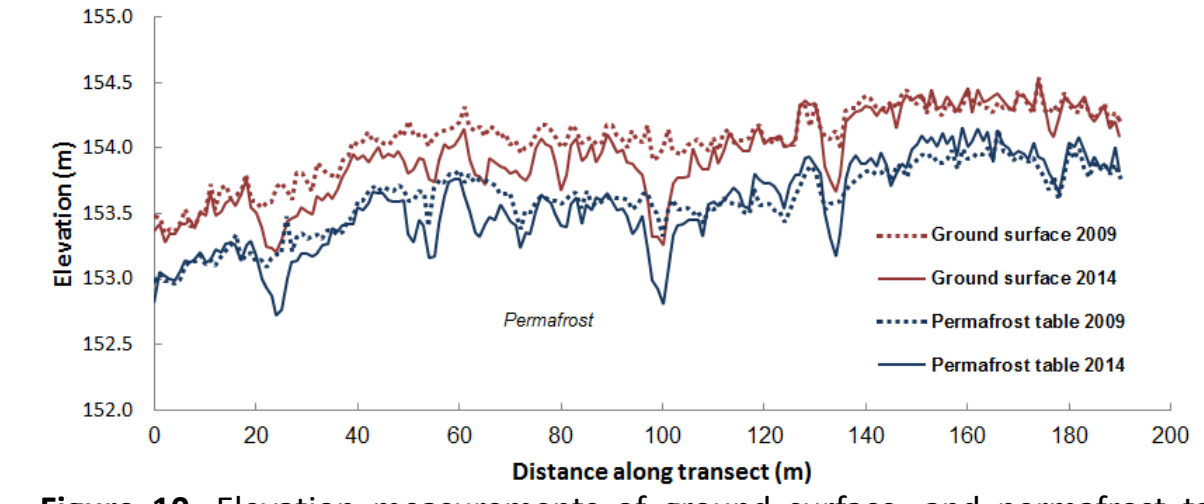


Figure 10. Elevation measurements of ground surface, and permafrost table from 2009–2014 in degrading ice-wedge terrain in yedoma soils near Umiat. Pit depths of > 1m are common; vegetation recovery is fastest in shallower pits.

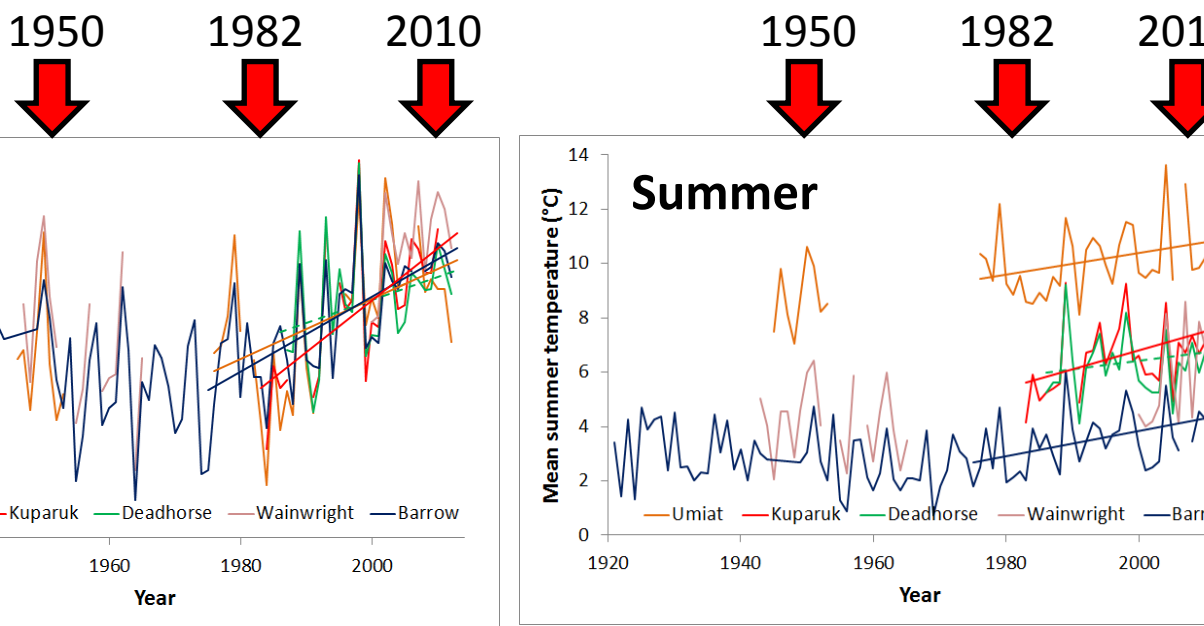


Fig. 11. North Slope met station data (1921–2012) indicate an upward trend in mean annual and summer (June–Aug) temperatures since the late 1970s, and there were several exceptionally warm years in the late 1990s and early 2000s. However, long-term observations at Barrow also indicate earlier warm periods. Warming since the end of the Little Ice Age could explain extensive degradation evident on the western North Slope by circa 1950.

Key Points

1. We quantified the extent of thaw pits in polygonal landscapes spanning the western and central North Slope in high-resolution imagery from circa 1950, 1982, and 2010.
2. Recent ice-wedge degradation across the North Slope cannot be explained by late 20th century warmth alone.
3. Ice-wedge degradation was already well-advanced at alluvio-marine deposits of Chukchi coastal plain by 1949. Changes since then primarily reflect stabilization of thaw pits.
4. Ice-wedge degradation began more recently on sand sheet and yedoma soils, especially at the eastern sites.
5. Early onset of degradation on western Chukchi coastal plain may have been triggered by earlier periods of warming after the Little Ice Age.

Literature Cited

Jorgenson, M T, Y L Shur, and E R Pullman. 2006. Abrupt increase in permafrost degradation in Arctic Alaska. *Geophysical Research Letters* 33:L02503.

Jorgenson, M T and J Grunblatt. 2013. Landscape-level ecological mapping of northern Alaska and field site photography. Report for Arctic Landscape Conservation Cooperative, U.S. Fish & Wildlife Service, Fairbanks, AK. 48 pp.

Jorgenson, M. T., M. Kanevskiy, Y. Shur, N. Moskalenko, D. R. N. Brown, K. Wickland, R. Striegl, and J. Koch (2015). Ground ice dynamics and ecological feedbacks control ice-wedge degradation and stabilization. *Journal of Geophysical Research–Earth Surface*. doi:10.1002/2015JF003602.

Liljedahl, A K, et al. Recent circum-Arctic ice-wedge degradation with major hydrologic impacts. *In revision, Nature–Geosciences*.

Raynolds M K, Walker D A, Ambrosius K J, Brown J, Everett K R, Kanevskiy M, Kofinas G P, Romanovsky V E, Shur Y, and Webber P J. 2014. Cumulative geocological effects of 62 years of infrastructure and climate change in ice-rich permafrost landscapes, Prudhoe Bay Oilfield, Alaska. *Global Change Biology* 20:1211–1224.

Shur, Y., K M Hinkel, and F E Nelson. 2005. The transient layer: implications for geocryology and climate-change science. *Permafrost and Periglacial Processes* 16:5–17.



Acknowledgements

Shell Exploration & Production Company funded this study as part of their multi-year Onshore Environmental Studies Program in northern Alaska.

